J Physiol (2003), **547.2**, *pp.* 543–553
DOI: 10.1113/jphysiol.2002.031005

www.jphysiol.org

Journal of Physiology

Modulation of AMPA receptors by cAMP-dependent protein kinase in preBötzinger complex inspiratory neurons regulates respiratory rhythm in the rat

Xuesi M. Shao, Qing Ge and Jack L. Feldman

Department of Neurobiology, David Geffen School of Medicine at UCLA, Los Angeles, CA 90095-1763, USA

We hypothesize that phosphorylation of AMPA receptors or associated synaptic proteins modulates the excitability of respiratory neurons in the preBötzinger Complex (preBötC), affecting respiratory rhythm. Using neonatal rat medullary slices that spontaneously generate respiratory rhythm, we examined the role of the cAMP–PKA pathway (PKA: cAMP-dependent protein kinase) in modulating glutamatergic synaptic transmission, the excitability of inspiratory neurons in the preBötC and respiratory rhythm. Microinjection of forskolin, an activator of adenylate cyclase, into the preBötC with or without the phosphodiesterase inhibitor 3-isobutyl-1-methylxanthine (IBMX), decreased the period (increased the frequency) of respiratory-related rhythmic motor output in the hypoglossal nerve (XIIn) to 84 % (without IBMX) and to 72 % (with IBMX) of the pre-injection baseline. In the presence of MK-801, a non-competitive NMDA receptor antagonist, microinjection of forskolin plus IBMX decreased the period to 66 % of baseline levels. Microinjection of Rp-adenosine 3′,5′-cyclic monophosphothioate (Rp-cAMPS), a PKA inhibitor, increased the period to 145 % of baseline levels. Concurrent microinjection of Rp-cAMPS and forskolin had no effect on the period. Bath application of 7β-deacetyl-7β-[γ-(morpholino)butyryl]-forskolin hydrochloride (7Db-forskolin, a water-soluble derivative of forskolin): (1) decreased the period to 67 % of baseline levels without affecting the amplitude of integrated XIIn inspiratory discharge, (2) induced a tonic inward current of 29 pA and enhanced inspiratory drive current (the amplitude increased to 183 % and the integral increased to 184 % of baseline) in voltage-clamped (holding potential = −60 mV) preBötC inspiratory neurons and (3) increased the frequency to 195 % and amplitude to 118 % of spontaneous excitatory postsynaptic currents (sEPSCs) during expiratory periods. Dideoxy-forskolin did not have these effects. Intracellular perfusion with the catalytic subunit of PKA (cPKA) into preBötC inspiratory neurons progressively enhanced inspiratory drive currents and, in the presence of TTX, increased the inward currents induced by local ejection of AMPA; the latter currents were blocked by 1,2,3,4-tetrahydro-6-nitro-2,3-dioxo-benzo[f]quinoxaline-7-sulphonamide (NBQX, an AMPA/kainate receptor antagonist). The effects of cPKA were blocked by co-application of PKA inhibitor (6–22) amide (PKI). These results suggest that phosphorylation of postsynaptic AMPA receptors through the cAMP–PKA pathway modulates both tonic and phasic excitatory amino acid synaptic transmission and excitability of inspiratory neurons in the preBötC and, therefore, regulates respiratory rhythm. Moreover, the basal level of endogenous PKA activity appears to be a determinant of resting respiratory frequency.

(Resubmitted 16 August 2002; accepted after revision 12 December 2002; first published online 24 January 2003)
Corresponding author X. M. Shao: Department of Neurobiology, Box 951763, David Geffen School of Medicine at UCLA, Los Angeles, CA 90095-1763, USA. Email: mshao@ucla.edu

The cAMP–PKA pathway mediates many actions of extracellular signals such as hormones and neurotransmitters on neuronal function. PKA phosphorylates cellular proteins such as ion channels and receptors. In particular, PKA modulates neuronal excitability and excitatory synaptic transmission through the phosphorylation of glutamate receptors (Greengard *et al.* 1991; Wang *et al.* 1991, 1993; Blackstone *et al.* 1994; Colwell & Levine, 1995; Roche *et al.* 1996; Traynelis & Wahl, 1997; Banke *et al.* 2000); for example, in hippocampal neurons, PKA potentiates the current induced by activation of non-NMDA glutamate receptors (Greengard *et al.* 1991; Wang *et al.* 1991). At the single-channel level, PKA increases the opening frequency and the mean open time of non-NMDA glutamate receptors (Greengard *et al.* 1991). PKA phosphorylates a serine site (Ser-845) at the C-terminal of GluR1, one of the subunits that form the pentameric AMPA receptor (Roche *et al.* 1996); phosphorylation of this site results in an increase of the peak open probability of AMPA receptors (Banke *et al.* 2000). The PKA

modulatory effects on postsynaptic AMPA receptors play a role in synaptic plasticity and have significant implications for network behaviour (Kameyama *et al.* 1998; Lee *et al.* 2000; Soderling & Derkach, 2000).

The preBötzinger complex (preBötC) in the rostroventrolateral medulla is hypothesized to contain neurons that generate respiratory rhythm in mammals (Smith *et al.* 1991; Rekling & Feldman, 1998; Gray *et al.* 1999). A medullary slice containing the preBötC can generate respiratory-related rhythmic motor output recorded from the XIIn (Smith *et al.* 1991). A subset of inspiratory neurons in the preBötC that are linked by excitatory synaptic connections (Rekling *et al.* 2000) is hypothesized to underlie respiratory rhythmogenesis (Rekling & Feldman, 1998; Koshiya & Smith, 1999). We have shown previously that excitatory glutamatergic neurotransmission mediated primarily by postsynaptic AMPA receptors is essential for respiratory rhythm generation in the respiratory-rhythmic slice (Funk *et al.* 1993; Ge & Feldman, 1998). In addition, modulation of AMPA receptors or associated synaptic proteins through phosphatase inhibition increases respiratory frequency, as well as the excitability of individual respiratory-related neurons in the preBötC (Ge & Feldman, 1998).

Here, we hypothesize that phosphorylation of AMPA receptors or associated synaptic proteins via the cAMP–PKA pathway modulates the excitability of respiratory neurons, modulates excitatory synaptic transmission in the preBötC, and therefore contributes to the regulation of respiratory rhythm. To test this hypothesis, we specifically examined in the respiratory-rhythmic slice: (1) the effects of activation of adenylate cyclase or inhibition of PKA in the preBötC on respiratory-related rhythmic motor output, (2) the effects of activation of adenylate cyclase on preBötC inspiratory neurons and on excitatory synaptic transmission and (3) the effects of activation of PKA on endogenous respiratory-related synaptic transmission and on exogenous AMPA-induced currents in preBötC inspiratory neurons.

METHODS

Slice preparation

All experiments on animals were carried out with the approval of the UCLA Institutional Animal Care and Use Committee. Experiments were performed on a medullary slice preparation that spontaneously generates respiratory rhythm (Smith *et al.* 1991). Briefly, neonatal Sprague-Dawley rats (0–3 days old) were anaesthetized by placing them on ice for at least 3 min. When they showed no reaction to noxious stimuli, the skull was rapidly opened. The cerebrum was separated from the brainstem with a lancet and destroyed. The brainstem–spinal cord was removed, pinned down with the ventral surface facing upward, mounted in the specimen vice of a Vibratome (VT 100, Technical Products International, MO, USA) and sectioned serially in the transverse plane until the nucleus ambiguus and inferior olivary nuclei were visible. One transverse slice (500–650 μm thick) containing the preBötC was then cut. The slice was transferred to a recording chamber of 3 ml volume and stabilized with a threaded frame. The dissection and slicing were performed in an artificial cerebrospinal fluid (ACSF) bubbled with 95 % O_2–5 % CO_2 at room temperature. The ACSF contained (mM): 128 NaCl, 3.0 KCl, 1.5 $CaCl_2$, 1.0 $MgSO_4$, 23.5 $NaHCO_3$, 0.5 NaH_2PO_4 and 30 glucose. During electrophysiological recording, the slice was continuously superfused (~3 ml min^{-1}) with ACSF (temperature maintained at 27 ± 1 °C) equilibrated with 95 % O_2–5 %CO_2. ACSF with increased KCl (9 mM) was used universally in these slice experiments as it results in a stable and long-lasting rhythmic motor output with a similar frequency and temporal pattern to the respiratory activities recorded from the fourth cervical ventral nerve root (C4) of the *en bloc* brainstem-spinal cord preparations (Smith *et al.* 1990, 1991).

Electrophysiological recording

Neurons within 100 μm of the top surface of the slice can be visualized with infrared-differential interference contrast (IR-DIC) microscopy (400X, Axioskop, Zeiss, Germany). The neurons we recorded fired in phase with the inspiratory bursts from XIIn and were located ventral to the nucleus ambiguus in the region of the preBötC (Smith *et al.* 1991). Patch electrodes were pulled from thick-wall borosilicate glass and had a tip size of 1–1.5 μm (resistance: 4–6.5 MΩ). The electrodes were filled with a solution containing (mM): 120 K-gluconate, 5.0 NaCl, 1.0 $CaCl_2$, 11 EGTA, 10 Hepes, 2.0 ATP (Mg^{2+} salt) and 2.0 ATP (dipotassium salt), pH adjusted to 7.3 using KOH. A positive pressure of 100–150 mmHg was applied to the back of the electrode as it was advanced into the tissue with a hydraulic micromanipulator. When the electrode was positioned on the surface of the soma of the target neuron, positive pressure was released and negative pressure was applied to form a gigaohm seal. The cell was then ruptured with short negative pressure pulses and/or with a voltage pulse from the patch-clamp amplifier. Intracellular signals were amplified with a patch-clamp amplifier (Axopatch 200A, Axon Instruments, CA, USA); whole-cell capacitance was compensated, as was the series resistance (80–90 %). Unless noted otherwise, during voltage-clamp recordings the neurons were held at −60 mV. A −10 mV junction potential was determined experimentally; reported values of potential are corrected values.

Respiratory-related nerve activity was recorded from the cut ends of XIIn with a suction electrode, amplified 10 000 or 20 000 times and band-pass filtered (1–3000 Hz) with an amplifier (P5 series, Grass Instruments, MA, USA). Signals from intracellular recording and from XIIn roots were recorded on videocassettes via pulse-code modulation (Vetter, PA, USA).

Drug application

Drugs were applied in four different ways: (1) bath application (i.e. adding them to the perfusate), (2) microinjection into the preBötC, (3) local application (ejecting them onto patch-clamped respiratory neurons) and (4) intracellular dialysis into neurons through the patch electrode. In microinjection experiments, pressure-injection pipettes (tip diameter 5–9 μm: pressure 0.6–1 kg cm^{-2}) were inserted into the preBötC 200–300 μm below the ventral surface of the slice. Injection volumes were determined by measuring the displacement of the pipette fluid meniscus with a microscope equipped with a calibrated eyepiece reticule. Slices were oriented so that the direction of superfusate flowed from dorsal to ventral to minimize the spread of drugs to neuronal populations dorsal to the preBötC (e.g. the hypoglossal motor nucleus). The pipette solution contained (mM) 142 NaCl, 9 KCl, 1.5 $CaCl_2$, 1.0 $MgSO_4$, 10 Hepes and 30 glucose, pH adjusted to 7.4 with NaOH. Forskolin, dideoxy-forskolin or 3-isobutyl-1-

methylxanthine (IBMX; a phosphodiesterase inhibitor) was dissolved in DMSO and then added to the solution to the final concentrations indicated in Results. The concentration of DMSO was < 2.5 %. Baseline measurements were taken immediately prior to drug application and responses were measured after responses had stabilized, 3–10 min after drug application, except in the intracellular dialysis experiments where measurements were made at specific time points after the formation of whole-cell recording (indicated in the figures). To avoid the residual effects of drugs confounding the results, only one or two (when co-injecting) drugs were injected into one preBötC. In a second group of experiments, injection of 2.5 % DMSO in the pipette solution was carried out as a control. For bath application experiments, only one drug (either 7Db-forskolin or dideoxy-forskolin) was applied in a given slice.

In the PKA dialysis experiments, cPKA or cPKA combined with PKI was applied intracellularly via dialysis from the patch-clamp electrode solution. To ensure dialysis of PKA, the access resistance of the electrodes was checked frequently. If the access resistance was high (> 30 MΩ) or unstable, the data was excluded.

The glutamate receptor agonist AMPA was dissolved in the pipette solution to 20 μM and applied locally onto patch-clamped neurons by pressure ejection. The ejection pipettes were mounted on a hydraulic micromanipulator and positioned in the tissue 30–40 μm away from the soma of the recorded neurons with the aid of an IR-DIC microscope. The tip size of the ejection pipette was 1–2 μm, and 0.6–1 kg cm^{-2} pressure was applied to the back of the pipette. In experiments with local application of AMPA, we first identified an inspiratory neuron in current- and voltage-clamp modes; then we added TTX (1 μM) to the bathing solution. Inspiratory burst activities of the neuron and the XIIn disappeared within 2–3 min. Approximately 4 min after the formation of whole-cell recording, we started to eject AMPA locally onto the recorded neuron. Peak AMPA-induced currents were measured immediately after pressure ejection of AMPA. The intervals between consecutive applications were at least 1.5 min to avoid the effects of desensitization.

Forskolin, 7Db-forskolin, 1,9-dideoxy forskolin, IBMX, 3′,5′-cyclic monophosphothioate (Rp-cAMPS triethylamine), (+)-MK-801 hydrogen maleate, (±)-AMPA hydrobromide, TTX, 1,2,3,4-tetrahydro-6-nitro-2,3-dioxo-benzo[f]quinoxaline-7-sulphonamide (NBQX) disodium, cPKA and PKI were obtained from Sigma/RBI (MO, USA).

Data analysis

Intracellular signals were low-pass filtered at 1 kHz with an eight-pole Bessel filter (Frequency Devices, MA, USA) and XIIn nerve activity was rectified and low-pass filtered (Paynter filter, τ=15 ms), then digitized at a sampling frequency of 4 kHz with Digidata 1200 hardware and Clampex 8 software (Axon Instruments) in a Pentium computer on- or off-line. For measuring the phasic inward current of inspiratory neurons, membrane current signals were filtered at 25 Hz and digitized at 100 Hz.

Respiratory periods were averaged from 10 consecutive periods in the baseline or drug-application conditions for each preparation. The amplitude of XIIn inspiratory bursts, the amplitude and area (integral) of the phasic inward currents of inspiratory neurons were measured from averaged envelope of 4–6 consecutive inspiratory periods triggered by the up-stroke of integrated inspiratory XIIn bursts (Clampex 8). The number of spikes (action potentials) and intra-burst frequency of spikes was averaged for 3–10 consecutive inspiratory bursts at each condition for each cell. They were then averaged across neurons or preparations and are presented as means ± S.D. The number of cells (for whole-cell recording) or preparations (for XIIn motor-output recording) is indicated by n. Paired t tests were used for determining the significance of differences between electrophysiological measurements during drug applications and pre-drug baseline measurements. Repeated-measures analysis of variance (ANOVA, Neter *et al.* 1990) was used to test the statistical significance of the time courses of the responses to intracellular dialysis with cPKA *vs.* controls. The procedure 'Mixed' from the data analysis software package SAS (V8) was used for this analysis (SAS Institute). The level of statistical significance was set at $P < 0.05$.

Spontaneous EPSCs (sEPSCs) during expiratory periods were detected by setting a threshold for the derivative of the membrane current signal. The time to peak and the peak amplitude of sEPSCs were measured. The neuronal activity and the time during inspiratory periods were ignored. The frequency of sEPSCs was calculated as the number of sEPSCs divided by total expiratory time over ~1 min of recording, and is expressed as the number of sEPSCs s^{-1}. The statistical significance of differences in rates (i.e. frequency of sEPSCs) was analysed with a method detailed in Shao & Feldman (2001). Since the amplitude of sEPSCs is not normally distributed, statistical significance for differences in sEPSC amplitude was analysed using the Kolmogorov-Smirnov test (Mini Analysis Program V5, Synaptosoft, GA, USA). The rates and the amplitudes of spontaneous EPSCs were tested during application of 7Db-forskolin and compared with the pre-forskolin baseline for each neuron.

RESULTS

Enhancement of cAMP–PKA activity in the preBötC increased respiratory frequency

In order to determine the effects of cAMP–PKA on the rhythm-generating network in the preBötC, we micro-injected forskolin (250–500 μM, 15–20 nl) into the preBötC unilaterally while recording the XIIn respiratory-related rhythmic motor output. Forskolin decreased respiratory period (increased frequency) from a pre-injection baseline of 7.3 ± 1.8 s to 6.0 ± 1.4 s (84 ± 10 % of pre-injection baseline, n = 6; Fig. 1*A* and *D*). Forskolin (100 μM) combined with IBMX (375 μM) decreased the respiratory period from 7.4 ± 3.5 s to 5.2 ± 2.2 s (72 ± 19 % of pre-injection baseline, n = 6). In the presence of MK-801 (100 μM), forskolin + IBMX decreased the respiratory period from 5.6 ± 1.6 s to 3.7 ± 1.3 s (66 ± 7 % of baseline, n = 4; Fig. 1*C* and *D*). The decrease in period occurred gradually at 2–5 min after the microinjection of forskolin with or without IBMX; this response remained relatively stable for 10–15 min, followed by a slight increase (Fig. 1*C*). In contrast, injection of the control solution with 2.5 % DMSO into the preBötC slightly increased the respiratory period (111 ± 18 % of baseline, not statistically significant. n = 5; Fig. 1*D*).

We then inhibited PKA by microinjection of Rp-cAMPS (0.5 mM, 15–20 nl), a membrane-permeable inhibitor of

PKA, into the preBötC; this increased the period of the XIIn rhythmic motor output from 5.4 ± 2.4 s to 7.5 ± 3.1 s (145 ± 47 % of baseline, $n = 11$; Fig. 1*B* and *D*). These changes occurred gradually at 2–4 min after Rp-cAMPS application and remained relatively stable for about 10–16 min. Co-injection of Rp-cAMPS (0.5 mM) and forskolin (0.5 mM) had no effect on respiratory period (100 ± 19 % of pre-injection baseline, $n = 3$).

Enhancement of cAMP–PKA activity potentiated excitatory neurotransmission in preBötC inspiratory neurons

To determine the neuronal mechanisms underlying the activation of PKA, we recorded preBötC inspiratory neurons in whole-cell patch-clamp mode and recorded the XIIn respiratory-related motor output simultaneously. PreBötC inspiratory neurons exhibit a rhythmic endogenous inspiratory drive potential and fire bursts of action potentials (under current-clamp) in phase with the inspiratory discharges in the XIIn (Smith *et al.* 1991); under voltage-clamp conditions, they exhibit phasic inspiratory inward currents. Bath application of 7Db-forskolin (50 μM) decreased the period to 67 ± 19 % of the pre-forskolin baseline, but did not affect the amplitude of integrated XIIn inspiratory discharge (106 ± 27 % of baseline, $n = 6$; Figs 2*A* and *B* and 3*A* and *E*; Table 1). In inspiratory neurons current-clamped to hold the baseline membrane potential at about −60 mV, 7Db-forskolin induced a depolarization. When we injected current to bring the membrane potential back to −60 mV, we observed an increase in amplitude and duration of the phasic inspiratory drive potential. The number of action potentials per inspiratory burst increased from 10.0 ± 4.7 burst^{-1} to 12.6 ± 5.2 burst^{-1} (133 ± 33 % of baseline, $n = 4$). The intra-burst frequency of action potentials also increased from 25.6 ± 13.7 s^{-1} to 34.5 ± 13.7 s^{-1} (149 ± 45 %, $n = 4$, Fig. 2*A*–*C*). Since in voltage-clamp mode the membrane potential can be held constant without interference by action potentials, we did further analysis with neurons voltage-clamped at −60 mV. Bath

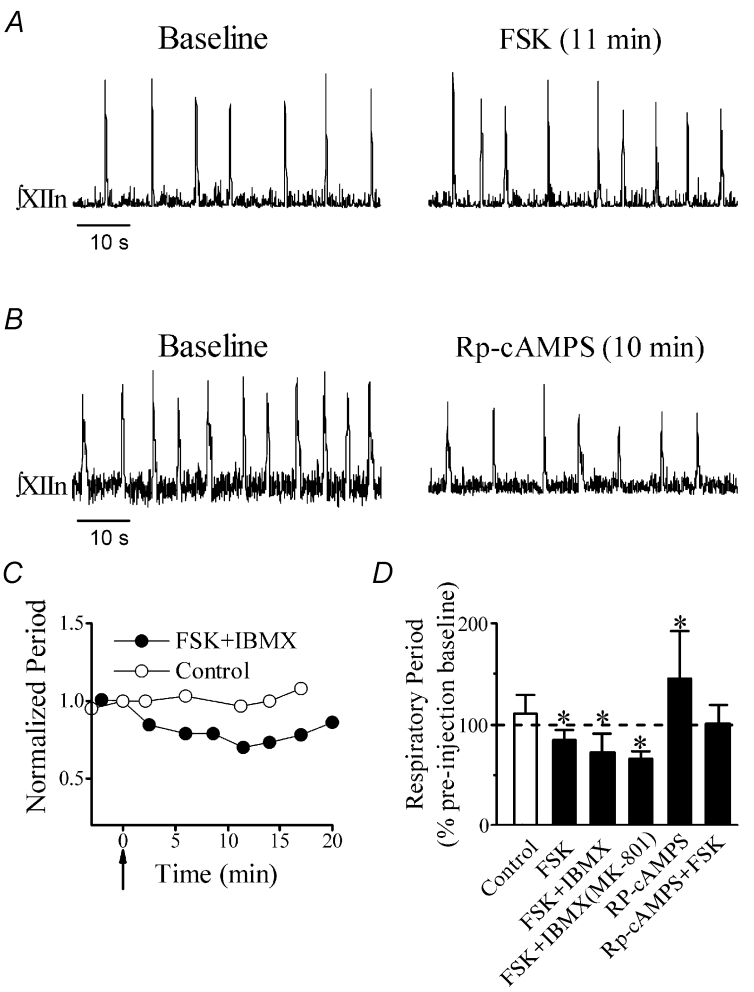

Figure 1. Activation of protein kinase A (PKA) in the preBötzinger complex (preBötC) increased the frequency of respiratory-related motor output, while its inhibition decreased the frequency

A, integrated hypoglossal nerve (XIIn) motor output (∫XIIn) before (Baseline) and 11 min after unilateral microinjection of 20 nl forskolin (FSK; 500 μM) into the preBötC. *B*, XIIn motor output before (Baseline) and 10 min after unilateral microinjection of 20 nl Rp-adenosine 3′,5′-cyclic monophosphothioate (Rp-cAMPS; 0.5 mM) into the preBötC. *C*, changes in the period of XIIn respiratory-related rhythmic motor output with time after microinjection of 15–20 nl FSK (100 μM) and 3-isobutyl-1-methylxanthine (IBMX; 375 μM) into the preBötC in the presence of 100 μM MK-801. Control indicates injection of solution containing 2.5 % DMSO. Each data point represents the normalized (dividing it by the baseline value immediately before injection) average of five consecutive periods of XIIn rhythmic motor output. The arrow indicates the starting time of the injection. *D*, summary of the effects. FSK (250–500 μM, $n = 6$), Rp-cAMPS (0.5 mM, $n = 11$) or a combination of Rp-cAMPS (0.5 mM) + FSK (0.5 mM; $n = 4$), each in volume of 15–20 nl, was injected into the preBötC. A combination of FSK (100 μM) + IBMX (375 μM) in a volume of 15–20 nl was injected into the preBötC in the presence ($n = 4$) or absence ($n = 6$) of MK-801 (100 μM) in the bath. The periods were determined by averaging 10 consecutive periods of XIIn rhythmic motor output for each condition with each preparation and then averaging across preparations, presented as mean ± S.D. percentage of the pre-injection baseline (period during drug application/period immediately before drug application). The hollow bar indicates the injection of control solution containing 2.5 % DMSO ($n = 5$). *Statistical significance ($P < 0.05$) tested by Student's paired *t* test on the raw data (non-normalized) taking drug application *vs.* pre-injection baseline in the same slice as pairs.

Table 1. Effects of 7Db-forskolin (7Db-FSK) *vs.* dideoxy-FSK on respiratory rhythm and preBötzinger complex (preBötC) inspiratory neurons

	Baseline	50 μM 7Db-FSK	Percentage of baseline	Baseline	50 μM Dideoxy-FSK	Percentage of baseline
XIIn motor output						
Respiratory period (s)	9.3 ± 3.1	6.2 ± 2.1*	67.3 ± 18.9	6.4 ± 0.9	6.4 ± 1.1	100.4 ± 7.3
Inspiratory amplitude (integrated) (μV)	89.3 ± 46.0	89.3 ± 41.9	105.8 ± 26.6	144.3 ± 38.0	135.3 ± 39.5	93.4 ± 8.8
PreBötC neurons						
Phasic inward current amplitude (pA)	30.7 ± 17.6	52.2 ± 25.4*	183.3 ± 80.6	39.3 ± 11.9	37.7 ± 11.5	96.1 ± 6.7
Phasic inward current integral (pA ms)	11324 ± 6676	20498 ± 12028*	183.5 ± 108.2	14525 ± 7292	12365 ± 5923	85.7 ± 6.9
Frequency of sEPSCs (s^{-1})†	3.6 ± 4.02	6.0 ± 6.85*	195.2 ± 74.2	2.0 ± 0.52	1.6 ± 0.43	87.0 ± 40.0
Amplitude of sEPSCs (pA)†	−19.4 ± 7.22	−22.5 ± 8.47*	118.4 ± 25.6	−20.5 ± 3.12	−19.2 ± 6.70	92.0 ± 22.2

Inspiratory amplitude (integrated) and phasic inward current amplitude were measured from the averaged envelope of 4–6 consecutive inspiratory periods triggered by the up-stroke of integrated inspiratory discharges from the hypoglossal nerve (XIIn) for each condition with each cell. The respiratory period was determined by averaging 10 consecutive periods for each condition with each preparation. The phasic inward current integral was the average of integrals of 4–6 consecutive periods measured as shape statistics 'Area' with Clampex 8 software (Axon Instrument). Then the data from different cells and different preparations were averaged and are presented as means ± S.D. *$P < 0.05$, Student's paired t test, drug *vs.* pre-drug baseline. † sEPSC indicates the spontaneous excitatory postsynaptic current during expiratory periods. The frequency of sEPSCs is the number of sEPSCs divided by total expiration time during ~1 min of recording. See Methods for the statistical tests for frequency and amplitude of sEPSCs. Statistical testing was carried out for 7Db-FSK or dideoxy-FSK *vs.* pre-drug baseline for every neuron. The frequency of sEPSCs increased significantly for all five neurons tested with 7Db-FSK. The difference in the frequency of sEPSCs was not significant for two of the three neurons tested with dideoxy-FSK, while for the other neuron, frequency decreased. The amplitude of sEPSCs increased significantly for four of the five neurons tested with 7Db-FSK. The difference in amplitude of sEPSCs was not significant for two of the three neurons tested with dideoxy-FSK, and for the other neuron, amplitude decreased.

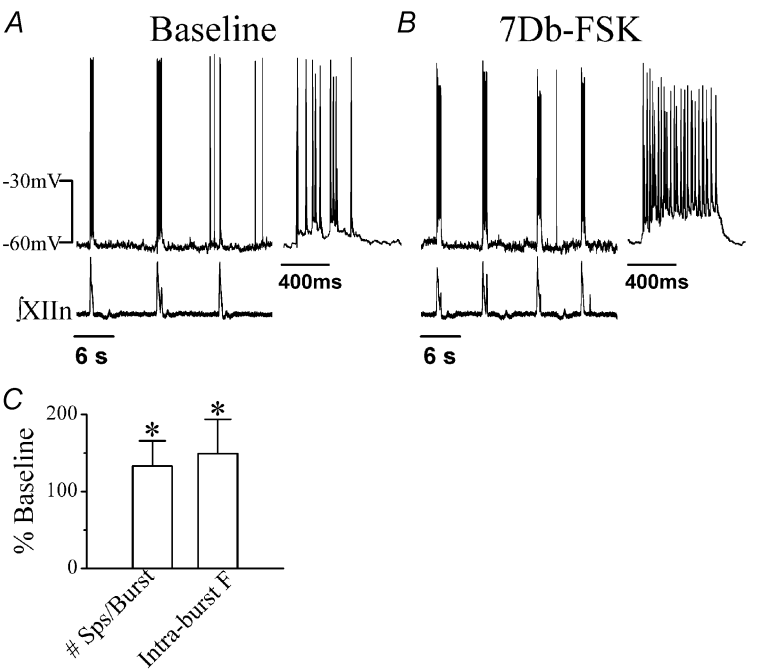

Figure 2. Effects of 7Db-forskolin (7Db-FSK) on inspiratory drive potential and bursts of preBötC inspiratory neurons

A, activity of an inspiratory neuron (current-clamped at −60 pA) and ∫XIIn in pre-drug baseline conditions. Inset: inspiratory burst corresponding to the first burst of the recording on the left on an extended time scale. *B*, activity of the neuron (current-clamped at −77 pA) and ∫XIIn during bath application of 50 μM 7Db-FSK. Inset: inspiratory burst corresponding to the first burst of the recording on the left in an extended time scale. *C*, the effects of bath application of 50 μM 7Db-FSK on mean spike number per inspiratory burst (#Sps/burst) and on intra-burst frequency of spikes (Intra-burst F). The data were averaged for 3–10 inspiratory bursts at the 7Db-FSK condition and at the pre-drug condition for each neuron and then averaged across neurons; presented as mean ± S.D. percentage of the pre-drug baseline ($n = 4$). *Statistical significance with paired t test (7Db-FSK *vs.* pre-drug) on the raw data (non-normalized).

application of 7Db-forskolin induced an inward current of 29 ± 31 pA (n = 5), increased the amplitude to 183 ± 81 % and increased the integral (area) to 184 ± 108 % of baseline of inspiratory drive currents (n = 6; Fig. 3*A* and *E*, Table 1). Application of 7Db-forskolin also increased the frequency of spontaneous EPSCs during expiratory periods to 195 ± 74 % of baseline and amplitude to118 ± 26 % of baseline (n = 5; Fig. 3*A*, *B* and *D*, Table 1). The statistical significance of the change in spontaneous EPSC frequency was tested with a method suggested by Shao & Feldman (2001, see Methods) comparing the frequencies during 7Db-forskolin application *vs.* pre-drug baseline for every neuron; the frequency increase was significant in five out of five neurons. We also tested the significance of the amplitude change with the Kolmogorov-Smirnov test; the amplitude increased significantly in four out of five neurons.

Since forskolin can act directly on ion channels in addition to activating adenylate cyclase, we performed control experiments with 1,9-dideoxy-forskolin, a structural analogue that does not stimulate adenylate cyclase but does mimic other actions of forskolin. Bath application of 50 μM dideoxy-forskolin did not increase respiratory frequency, induce any inward current, enhance the amplitude or the integral of inspiratory drive current in voltage-clamped preBötC inspiratory neurons and did not increase the frequency or the amplitude of spontaneous EPSCs (Fig. 3*C* and *E*; Table 1; n = 3).

PKA enhanced endogenous inspiratory drive and exogenous AMPA-induced currents in preBötC inspiratory neurons

The enhancement of neuronal excitability observed during bath application of forskolin, in addition to the direct effects of activating adenylate cyclase in inspiratory neurons, could be due to indirect effects through actions of forskolin on neurons that projected to the recorded neurons. In order to demonstrate the role of PKA on the excitability of preBötC inspiratory neurons, cPKA (200 U ml^{-1}) was applied intracellularly via dialysis from the patch-clamp electrode solution. cPKA increased the amplitude of the inspiratory drive potential in current-clamped inspiratory neurons (maintaining the expiratory period membrane voltage at ~−60 mV, Fig. 4*A*). We carried out a detailed analysis of inspiratory drive currents with neurons voltage-clamped at −60 mV. The amplitude of peak inspiratory drive currents increased from 102 ± 93 pA (n = 7) measured immediately after the establishment of whole-cell recording conditions to

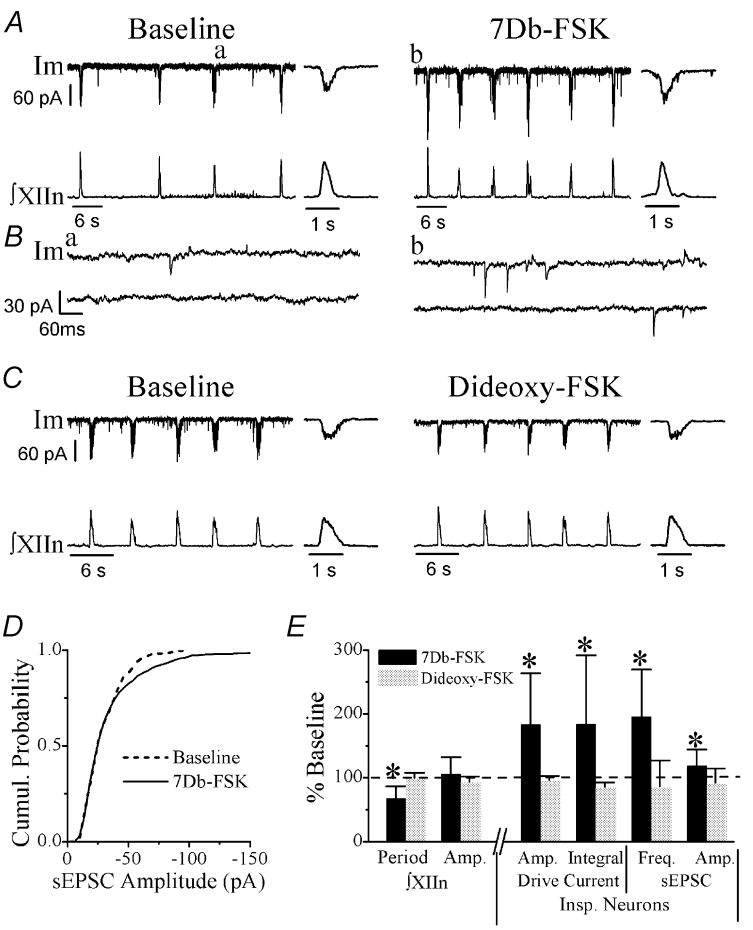

Figure 3. Effects of 7Db-FSK *vs.* dideoxy-FSK on respiratory rhythm and preBötC inspiratory neurons

A, membrane current (I_m) of an inspiratory neuron (voltage-clamped at −60 mV) and ∫XIIn before (Baseline) and during bath application of 50 μM 7Db-FSK. Insets: average of five consecutive inspiratory drive currents and ∫XIIn inspiratory discharges on an extended time scale. *B*, examples of spontaneous EPSCs (sEPSCs) on an extended time scale. a and b correspond to a and b in panel *A*. *C*, I_m of another inspiratory neuron and ∫XIIn before (Baseline) and during bath application of 50 μM dideoxy-FSK. Insets: average of five consecutive inspiratory drive currents and ∫XIIn inspiratory discharges on an extended time scale. *D*, cumulative histogram of sEPSC amplitude of a representative example neuron before (Baseline, 485 events in ~1 min of recording) and during (712 events in ~1 min of recording) bath application of 50 μM 7Db-FSK. The difference in sEPSC amplitude between the two conditions is significant (Kolmogorov-Smirnov test, P = 0.031). *E*, summary of the effects of 7Db-FSK and dideoxy-FSK on respiratory period and the amplitude (Amp.) of ∫XIIn activity, on the amplitude and integral of phasic inspiratory drive currents as well as on the frequency (Freq.) and amplitude of sEPSCs (mean ± S.D. of n = 6 for 7Db-FSK, n = 3 for Dideoxy-FSK). *Significant at $P < 0.05$ (Student's paired t test on the raw data (not normalized) taking drug application *vs.* pre-drug baseline at the same neurons as pairs). See Methods and Results for details of the statistical tests for frequency and amplitude of sEPSC.

136 ± 100 pA after 40 min of recording (with cPKA in the patch electrode; Fig. 4*B*). An increase in the integral (area) of inspiratory drive currents (i.e. total charge transfer) was also observed ($n = 7$; Fig. 4*C*). To confirm that these modulatory effects on inspiratory drive currents resulted from activation of the PKA pathway by cPKA, we performed two control experiments: a null control with a patch-electrode solution without cPKA, the other with the patch electrode solution containing 200 U ml^{-1} cPKA + 500 μg ml^{-1} PKI, a potent inhibitor of PKA (Glass *et al.* 1989; Roche *et al.* 1996). Neither the amplitude nor integral of inspiratory drive current increased over time in either control experiment ($n = 4$ for each condition; Fig. 4*B* and *C*). We analysed the effects of cPKA on the peak and the integral of inspiratory drive currents with a two-way repeated-measures ANOVA model. The estimates of the slopes of the three groups indicated that the increase in peak inspiratory drive currents over time in the cPKA group was significant, but the changes in peak inspiratory drive currents in the other two groups were not. The differences in the time course of the changes in the peak inspiratory drive currents between the experimental group with the cPKA and the two control groups were highly significant ($P = 0.0001$). *Post hoc* pairwise comparisons

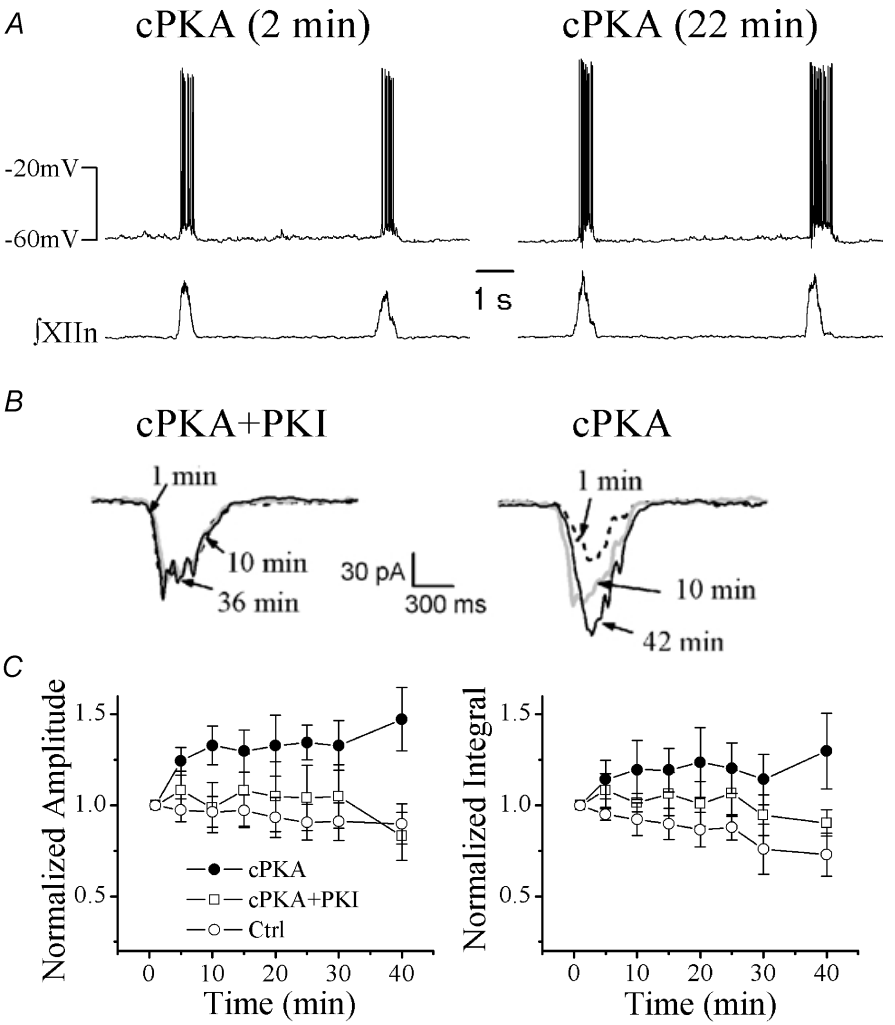

Figure 4. Intracellular dialysis with the catalytic subunit of PKA (cPKA) enhanced endogenous inspiratory drive in preBötC inspiratory neurons

A, inspiratory drive potential in a cPKA-dialysed (200 U ml^{-1}) inspiratory neuron (current clamp at −15 pA) at 2 min (left) and at 22 min (right) after formation of whole-cell recording. *B*, averages of five consecutive inspiratory drive currents (voltage clamped at −60 mV) of a neuron dialysed with cPKA (200 U ml^{-1}) + PKA inhibitor 6–22 amide (PKI, 500 μg ml^{-1}; left panel) and of another neuron dialysed with cPKA (200 U ml^{-1}) alone at different time points indicated after the formation of whole-cell recording. *C*, time courses of peak amplitude and integral (normalized to the value at the beginning of whole cell recording for each neuron, mean ± S.E.M.) of inspiratory drive currents in neurons dialysed with 200 U ml^{-1} cPKA ($n = 7$), cPKA (200 U ml^{-1}) + PKI (500 μg ml^{-1}; $n = 4$) and null control solution ($n = 4$). The changes in peak amplitude and integral over time between cPKA and control groups were statistically significant, as tested by two-way repeated-measures ANOVA. They were not significant between cPKA + PKI and null control groups.

indicated that the time course of the changes in the peak current of the cPKA group was significantly different from the null control, significantly different from the cPKA + PKI group, while that of the cPKA + PKI group was not significantly different from the null control (Fig. 4*C*, left panel). Similarly, the estimates of the slopes indicated that the increase in the integral of inspiratory drive currents over time in the cPKA group was significant; the decrease in the integral over time in the null control group was significant, while the change in the cPKA + PKI group was not significant. The differences in the time courses of the changes in the integral of inspiratory drive currents between the experimental group with the cPKA and the two control groups were highly significant ($P = 0.0003$). *Post hoc* pairwise comparisons indicated that the time course of the changes in the integral of the cPKA group was significantly different from the null control, and from the cPKA + PKI group, while that of cPKA + PKI group was not significantly different from the null control (Fig. 4*C*, right panel).

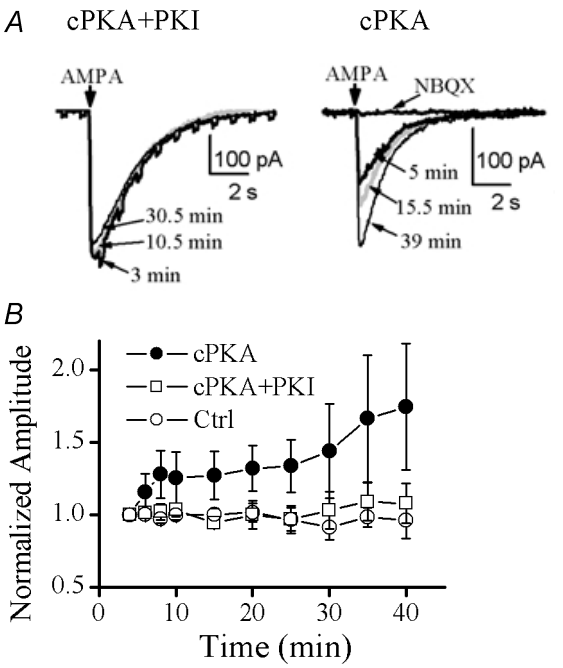

Figure 5. Intracellular dialysis with cPKA enhanced exogenous AMPA-induced currents in preBötC inspiratory neurons

A, local ejections of 20 μM AMPA induced inward currents in a voltage-clamped (at −60 mV) inspiratory neuron dialysed with cPKA (200 U ml^{-1}) + PKI (500 μg ml^{-1}; left panel) and another neuron dialysed with cPKA (200 U ml^{-1}; right panel). TTX (1 μM) was present in the bath solution. The arrows indicate the time when a 150 ms pressure pulse was applied to the ejection pipette. The currents measured at the different time points indicated after the formation of whole-cell recording were superimposed. An increase in membrane conductance, associated with the currents, was illustrated by a series of −5 mV voltage pulses applied to the voltage-clamped neuron (current trace measured at 3 min in the left panel). This AMPA-induced current could be blocked by bath application of 5 μM 1,2,3,4-tetrahydro-6-nitro-2,3-dioxo-benzo[f]quinoxaline-7-sulphonamide (NBQX; right panel). *B*, time courses of AMPA-induced current amplitude (mean ± S.E.M.; normalized to the values at about 4 min from the beginning of whole-cell recordings when TTX took effect) in inspiratory neurons dialysed with cPKA (200 U ml^{-1}; $n = 6$), cPKA (200 U ml^{-1}) + PKI (500 μg ml^{-1}; $n = 3$) and null control solution ($n = 3$). The changes in amplitude over time between cPKA and control groups were significant, as tested by two-way repeated-measures ANOVA. They were not significant between cPKA + PKI and null control groups.

To examine further the effects of increasing intracellular PKA on AMPA receptor function, with 1 μM TTX in the bath we pressure ejected AMPA (20 μM, 100–200 ms pressure pulse) onto inspiratory neurons (identified as such before the application of TTX). Local ejection of AMPA induced an inward current of 289 ± 157 pA associated with an increase in whole-cell conductance immediately after TTX blocked action potential generation. With the patch electrode containing 200 U ml^{-1} cPKA, the AMPA-induced currents increased with time in these neurons (469 ± 335 pA at 40 min after the formation of whole-cell recording, $n = 6$; Fig. 5*A* and *B*). The AMPA-induced inward current was completely abolished by bath application of the non-NMDA glutamate receptor antagonist NBQX (5 μM; Fig. 5*A*). Under the two control conditions, where patch electrodes contained standard patch solution without cPKA or patch electrodes solution containing cPKA (200 U ml^{-1}) + PKI (500 μg ml^{-1}), no increase in AMPA-induced current was observed (Fig. 5*A* and *B*). The effects of cPKA on the AMPA-induced current measured at a series of time points from the formation of whole-cell recording (Fig. 5*B*) were analysed with a two-way repeated-measures ANOVA model. The estimates of the slopes indicated that the increase in AMPA-induced current over time in the cPKA group was significant, while the changes in AMPA-induced current over time in the other two groups were not significant. The model also indicated that the differences in the time courses of the changes in the peak AMPA-induced currents between the cPKA group and the two control groups were highly significant ($P = 0.0001$). *Post hoc* pairwise comparisons indicated that the time course of the changes in the peak current of the cPKA group was significantly different from the null control, significantly different from the cPKA + PKI group, while that of the cPKA + PKI group was not significantly different from the null control.

DISCUSSION

Phosphorylation of postsynaptic AMPA receptors (or associated synaptic proteins) by PKA plays a role in modulating synaptic strength and in synaptic plasticity in many brain structures including the CA1 region of hippocampus, the neostriatum and the cerebral cortex (Blackstone *et al.* 1994; Colwell & Levine, 1995; Kameyama *et al.* 1998; Lee *et al.* 2000; Soderling & Derkach, 2000). In

this study we show that manipulating PKA activity in the preBötC modulates respiratory rhythm in neonatal rat medullary slice preparations. Enhancement of PKA activity in the preBötC increased the frequency of respiratory-related rhythmic motor output, while inhibition of PKA activity decreased the frequency. This suggests that the basal level of phosphorylation plays a role in the determination of baseline respiratory frequency. In preBötC inspiratory neurons, enhancement of PKA activity induced a tonic inward current, increased the frequency and amplitude of spontaneous EPSCs, increased the endogenous inspiratory drive currents, as well as the exogenous AMPA-induced currents. Our results suggest that PKA modulates the excitability of preBötC inspiratory neurons and excitatory synaptic transmission through phosphorylation of AMPA receptors or related synaptic proteins; these changes in preBötC neurons may underlie the modulation of respiratory rhythm.

The preBötC is hypothesized to be the site for respiratory rhythm generation in mammals (Smith *et al.* 1991), with a subset of preBötC inspiratory neurons underlying rhythmogenesis (Rekling & Feldman, 1998; Gray *et al.* 1999). If the excitability of neurons involved in rhythmogenesis in the preBötC is enhanced, we would expect an increase in respiratory frequency (Rekling & Feldman, 1998; Butera *et al.* 1999). Microinjection into the preBötC of forskolin or co-injection with a phosphodiesterase inhibitor to elevate intracellular cAMP concentration increased the frequency of the XIIn respiratory-related rhythmic motor output; injection of an inhibitor of PKA decreased the frequency (Fig. 1). During bath application of 7DB-forskolin, the excitability of inspiratory neurons in the preBötC was enhanced and the frequency of the XIIn inspiratory discharges increased (Figs 2 and 3), while the amplitude of these discharges remained constant. These observations are consistent with the preBötC site hypothesis. The effects of forskolin on inspiratory neurons and on respiratory rhythm are likely to be mediated by the activation of adenylate cyclase, since the inactive analogue dideoxy-forskolin did not induce any similar response, and these effects were blocked by co-injection of Rp-CAMPS (Figs 1*D* and 3*C* and *E*). These results are consistent with our previous report that phosphatase inhibition increases respiratory frequency, as well as the excitability of individual respiratory-related neurons in the preBötC (Ge & Feldman, 1998).

Coupled glutamatergic inspiratory neurons are hypothesized to be the kernel of respiratory rhythm generation (Rekling & Feldman, 1998). Both the excitatory synaptic coupling between inspiratory neurons and the tonic excitatory input to inspiratory neurons in the preBötC are proposed to be glutamatergic, mediated primarily by non-NMDA glutamate receptors (Funk *et al.* 1993; Ge & Feldman, 1998). Both phasic inspiratory current and spontaneous EPSCs during expiratory periods can be completely abolished by 6-cyano-7-nitroquinoxaline-2,3-dione (CNQX) (Shao & Feldman, 2001). In preBötC inspiratory neurons, bath application of forskolin increased the frequency and amplitude of spontaneous EPSCs and induced a tonic inward current; this suggests that enhancement of PKA activity increases neuronal excitability by potentiating tonic excitatory synaptic transmission. Forskolin also increased the peak and the integral of inspiratory drive current in these neurons (Fig. 3 and Table 1), suggesting an enhancement of phasic excitatory synaptic transmission. The effects of bath application of 7Db-forskolin can be attributed to the modulation of postsynaptic non-NMDA glutamate receptors in inspiratory neurons as well as the enhancement of the excitability of those neurons that provide tonic and/or phasic excitatory input to the neurons we recorded. Postsynaptic effects related to changes in AMPA receptor function were confirmed, since dialysis with cPKA into individual preBötC inspiratory neurons increased the phasic inspiratory drive current and, in the presence of TTX, resulted in enhancement of the AMPA-induced current. These results do not exclude the possibility that presynaptic mechanisms are also involved in the modulation of synaptic transmission by cAMP–PKA activity (Chavez-Noriega & Stevens, 1994; Evans *et al.* 2001).

PKA induces potentiation of glutamate or kainate-activated currents in hippocampal neurons and human embryonic kidney cells expressing glutamate receptor subunit 6 (GluR6) (Greengard *et al.* 1991; Wang *et al.* 1993). Since kainate receptors are present in preBötC respiratory neurons (Ge & Feldman, 1998) and kainate receptors can be phosphorylated by PKA (Wang *et al.* 1991, 1993; Traynelis & Wahl, 1997), we are not able to exclude the possibility that activation of PKA also phosphorylates kainate receptors in preBötC inspiratory neurons. However, since AMPA receptors are the principal mediators of the excitatory synaptic transmission underlying rhythm generation within the preBötC (Funk *et al.* 1993; Ge & Feldman, 1998) and we observed that enhancement of PKA activity potentiated the AMPA-induced current in preBötC inspiratory neurons, we postulate that the modulatory effects of PKA on respiratory rhythm are primarily due to phosphorylation of AMPA receptors or related synaptic proteins mediating excitatory synaptic transmission.

NMDA receptors can be modulated by phosphorylation through the cAMP–PKA pathway (Colwell & Levine, 1995; Snyder *et al.* 1998; Nijholt *et al.* 2000). Since NMDA receptor-mediated synaptic transmission is not essential for respiratory rhythm generation under our experimental conditions (Funk *et al.* 1993, 1997) and the frequency modulation effects of microinjection of forskolin and IBMX persisted after blockade of NMDA receptors by

MK-801 (Fig. 1*C* and *D*), the obligatory involvement of NMDA receptor phosphorylation in respiratory rhythm modulation would be minimal.

Respiration in mammals is a behaviour that is modulated continuously for regulation of blood gases and for coordination with other movements, such as swallowing, phonation and locomotion. The pattern of breathing is regulated by numerous neuromodulatory inputs to the respiratory rhythm generation network. G-protein-coupled receptors such as muscarinic acetylcholine, tachykinin (substance P), serotonin, thyrotropin-releasing hormone (TRH), μ-opioid, α-adrenergic and $GABA_B$ receptors are involved in the modulation of respiratory frequency (Murakoshi *et al.* 1985). Activation of these receptors in the preBötC regulates respiratory frequency and amplitude (Johnson *et al.* 1996; Rekling *et al.* 1996; Gray *et al.* 1999; Shao & Feldman, 2000). Among these receptors, activation of muscarinic, tachykinin, TRH, serotonin, μ-opioid and $GABA_B$ receptors affects the cAMP–PKA pathway in neurons (Wojcik & Neff, 1984; Felder, 1995; Khawaja & Rogers, 1996; Lukyanetz & Kostyuk, 1996; Oka *et al.* 1996; Deisz, 1997; Nestler, 1997; Badie-Mahdavi *et al.* 2001; Browning & Travagli, 2001; Cai *et al.* 2002). We speculate that the endogenous neuromodulators acting on these receptors continuously modulate cAMP levels in preBötC rhythmogenic neurons, which serves to maintain respiratory homeostasis in response to changes in state (e.g. sleep *vs.* wakefulness, exercise, pregnancy and disease). The question as to which G-protein-coupled receptors link to the cAMP–PKA pathway in preBötC rhythmogenic neurons remains to be elucidated.

In summary, we have demonstrated the role of the cAMP–PKA pathway in regulating respiratory rhythm in the neonatal rat. We suggest that PKA is an endogenously active kinase that modulates AMPA-receptor-mediated respiratory-related currents (both phasic and tonic) in preBötC inspiratory neurons and therefore modulates the breathing rhythm.

REFERENCES

Badie-Mahdavi H, Worsley MA, Ackley MA, Asghar AU, Slack JR & King AE (2001). A role for protein kinase intracellular messengers in substance P- and nociceptor afferent-mediated excitation and expression of the transcription factor Fos in rat dorsal horn neurons *in vitro*. *Eur J Neurosci* **14**, 426–434.

Banke TG, Bowie D, Lee H, Huganir RL, Schousboe A & Traynelis SF (2000). Control of GluR1 AMPA receptor function by cAMP-dependent protein kinase. *J Neurosci* **20**, 89–102.

Blackstone C, Murphy TH, Moss SJ, Baraban JM & Huganir RL (1994). Cyclic AMP and synaptic activity-dependent phosphorylation of AMPA-preferring glutamate receptors. *J Neurosci* **14**, 7585–7593.

Browning KN & Travagli RA (2001). The peptide TRH uncovers the presence of presynaptic 5-HT1A receptors via activation of a second messenger pathway in the rat dorsal vagal complex. *J Physiol* **531**, 425–435.

Butera R, Rinzel J & Smith J (1999). Models of respiratory rhythm generation in the pre-Bötzinger complex. II. Populations of coupled pacemaker neurons. *J Neurophysiol* **82**, 398–451.

Cai X, Flores-Hernandez J, Feng J & Yan Z (2002). Activity-dependent bidirectional regulation of GABA(A) receptor channels by the 5-HT(4) receptor-mediated signalling in rat prefrontal cortical pyramidal neurons. *J Physiol* **540**, 743–759.

Chavez-Noriega LE & Stevens CF (1994). Increased transmitter release at excitatory synapses produced by direct activation of adenylate cyclase in rat hippocampal slices. *J Neurosci* **14**, 310–317.

Colwell CS & Levine MS (1995). Excitatory synaptic transmission in neostriatal neurons: regulation by cyclic AMP-dependent mechanisms. *J Neurosci* **15**, 1704–1713.

Deisz RA (1997). Electrophysiology of $GABA_B$ receptors. In *The GABA Receptors*, ed. Enna SJ & Bowery NG, pp. 157–207. Humana, Totowa, New Jersey.

Evans DI, Jones RS & Woodhall G (2001). Differential actions of PKA and PKC in the regulation of glutamate release by group III mGluRs in the entorhinal cortex. *J Neurophysiol* **85**, 571–579.

Felder CC (1995). Muscarinic acetylcholine receptors: signal transduction through multiple effectors. *FASEB J* **9**, 619–625.

Funk GD, Johnson SM, Smith JC, Dong XW, Lai J & Feldman JL (1997). Functional respiratory rhythm generating networks in neonatal mice lacking NMDAR1 gene. *J Neurophysiol* **78**, 1414–1420.

Funk GD, Smith JC & Feldman JL (1993). Generation and transmission of respiratory oscillations in medullary slices: role of excitatory amino acids. *J Neurophysiol* **70**, 1497–1515.

Ge Q & Feldman JL (1998). AMPA receptor activation and phosphatase inhibition affect neonatal rat respiratory rhythm generation. *J Physiol* **509**, 255–266.

Glass DB, Cheng HC, Mende-Mueller L, Reed J & Walsh DA (1989). Primary structural determinants essential for potent inhibition of cAMP-dependent protein kinase by inhibitory peptides corresponding to the active portion of the heat-stable inhibitor protein. *J Biol Chem* **264**, 8802–8810.

Gray PA, Rekling JC, Bocchiaro CM & Feldman JL (1999). Modulation of respiratory frequency by peptidergic input to rhythmogenic neurons in the preBötzinger complex. *Science* **286**, 1566–1568.

Greengard P, Jen J, Nairn AC & Stevens CF (1991). Enhancement of the glutamate response by cAMP-dependent protein kinase in hippocampal neurons. *Science* **253**, 1135–1138.

Johnson SM, Smith JC & Feldman JL (1996). Modulation of respiratory rhythm *in vitro*: role of Gi/o protein-mediated mechanisms. *J Appl Physiol* **80**, 2120–2133.

Kameyama K, Lee HK, Bear MF & Huganir RL (1998). Involvement of a postsynaptic protein kinase A substrate in the expression of homosynaptic long-term depression. *Neuron* **21**, 1163–1175.

Khawaja AM & Rogers DF (1996). Tachykinins: receptor to effector. *Int J Biochem Cell Biol* **28**, 721–738.

Koshiya N & Smith JC (1999). Neuronal pacemaker for breathing visualized *in vitro*. *Nature* **400**, 360–363.

Lee HK, Barbarosie M, Kameyama K, Bear MF & Huganir RL (2000). Regulation of distinct AMPA receptor phosphorylation sites during bidirectional synaptic plasticity. *Nature* **405**, 955–959.

Lukyanetz EA & Kostyuk PG (1996). Two distinct receptors operate the cAMP cascade to up-regulate L-type Ca channels. *Pflugers Arch* **432**, 174–181.

Murakoshi T, Suzue T & Tamai S (1985). A pharmacological study on respiratory rhythm in the isolated brainstem-spinal cord preparation of the newborn rat. *Br J Pharmacol* **86**, 95–104.

Nestler EJ (1997). Molecular mechanisms of opiate and cocaine addiction. *Curr Opin Neurobiol* **7**, 713–719.
Neter J, Wasserman W & Kutner MH (ed.) (1990). Repeated measures and related designs. In *Applied Linear Statistical Models*, pp. 1035–1073. Irwin, Homewood, IL.
Nijholt I, Blank T, Liu A, Kügler H & Spiess J (2000). Modulation of hypothalamic NMDA receptor function by cyclic AMP-dependent protein kinase and phosphatases. *J Neurochem* **75**, 749–754.
Oka M, Itoh Y, Ukai Y, Yoshikuni Y & Kimura K (1996). Protein kinases are involved in prolonged acetylcholine release from rat hippocampus induced by thyrotropin-releasing hormone analogue NS-3. *J Neurochem* **66**, 1889–1893.
Rekling JC, Champagnat J & Denavit-Saubié M (1996). Thyrotropin-releasing hormone (TRH) depolarizes a subset of inspiratory neurons in the newborn mouse brain stem *in vitro*. *J Neurophysiol* **75**, 811–819.
Rekling JC & Feldman JL (1998). PreBötzinger complex and pacemaker neurons: hypothesized site and kernel for respiratory rhythm generation. *Annu Rev Physiol* **60**, 385–405.
Rekling JC, Shao XM & Feldman JL (2000). Electrical coupling and excitatory synaptic transmission between rhythmogenic respiratory neurons in the preBötzinger complex. *J Neurosci* **20**, RC113.
Roche KW, O'Brien RJ, Mammen AL, Bernhardt J & Huganir RL (1996). Characterization of multiple phosphorylation sites on the AMPA receptor GluR1 subunit. *Neuron* **16**, 1179–1188.
Shao XM & Feldman JL (2000). Acetylcholine modulates respiratory pattern: effects mediated by M3-like receptors in preBötzinger complex inspiratory neurons. *J Neurophysiol* **83**, 1243–1252.
Shao XM & Feldman JL (2001). Mechanisms underlying regulation of respiratory pattern by nicotine in preBötzinger Complex. *J Neurophysiol* **85**, 2461–2467.
Smith JC, Ellenberger HH, Ballanyi K, Richter DW & Feldman JL (1991). Pre-Bötzinger complex: a brainstem region that may generate respiratory rhythm in mammals. *Science* **254**, 726–729.
Smith JC, Greer JJ, Liu GS & Feldman JL (1990). Neural mechanisms generating respiratory pattern in mammalian brain stem-spinal cord *in vitro*. I. Spatiotemporal patterns of motor and medullary neuron activity. *J Neurophysiol* **64**, 1149–1169.
Snyder GL, Fienberg AA, Huganir RL & Greengard P (1998). A dopamine/D1 receptor/protein kinase A/dopamine- and cAMP-regulated phosphoprotein (Mr 32 kDa)/protein phosphatase-1 pathway regulates dephosphorylation of the NMDA receptor. *J Neurosci* **18**, 10297–10303.
Soderling TR & Derkach VA (2000). Postsynaptic protein phosphorylation and LTP. *Trends Neurosci* **23**, 75–80.
Traynelis SF & Wahl P (1997). Control of rat GluR6 glutamate receptor open probability by protein kinase A and calcineurin. *J Physiol* **503**, 513–531.
Wang LY, Salter MW & MacDonald JF (1991). Regulation of kainate receptors by cAMP-dependent protein kinase and phosphatases. *Science* **253**, 1132–1135.
Wang LY, Taverna FA, Huang XP, MacDonald JF & Hampson DR (1993). Phosphorylation and modulation of a kainate receptor (GluR6) by cAMP-dependent protein kinase. *Science* **259**, 1173–1175.
Wojcik WJ & Neff NH (1984). gamma-aminobutyric acid B receptors are negatively coupled to adenylate cyclase in brain, and in the cerebellum these receptors may be associated with granule cells. *Mol Pharmacol* **25**, 24–28.

Acknowledgements
The authors thank Dr Shane Saywell for valuable comments on the manuscript. This study is supported by NIH grants (HL40959 and NS24742), Tobacco-Related Disease Research Program (California) grant no. 10RT-0241 and an American Lung Association of California Research Training Fellowship to QG.

Present address
Q. Ge: University of Tennessee Medical Center, Department of Medicine, 1924 Alcoa Highway, Knoxville, Tennessee 37920, USA.